High-Q Self-Resonant Structure for Wireless Power Transfer

Aaron L.F. Stein Phyo Aung Kyaw Charles R. Sullivan
Thayer School of Engineering
Dartmouth College
Hanover, NH 03755 USA
Email: {Aaron.L.Stein, Phyo.A.Kyaw.TH, Charles.R.Sullivan}@dartmouth.edu

***Abstract*—The range and efficiency of wireless power transfer systems are limited by the quality factor of the transmit and receive coils used. Multi-layer self-resonant structures have been proposed as a low-cost method for creating high-Q coils for high-frequency wireless power transfer. In these structures thin foil layers are separated by a dielectric material in order to form a capacitance that resonates with the inductance of the structure, while also forcing equal current sharing between conductors. In order to reduce winding loss, these structures are made with foil layers much thinner than a skin depth, which makes the layers of the structure extremely difficult to handle. In this paper, we present a modified self-resonant structure in which the layered conductors are made from standard PCB substrates with no vias. The PCB substrates provide an inexpensive way to handle thin conductive layers, and the modified self-resonant structure ensures that the poor dielectric properties of the PCB substrates do not impact the quality factor of the structure. The modified self-resonant structure makes it feasible to achieve advantages similar to litz wire, but at multi-MHz frequencies where effective litz wire is not commercially available. Experimental results show that the structure has a quality factor of 1177 at 7.08 MHz, despite only being 6.6 cm in diameter. The quality factor normalized by the diameter is more than 6.5x larger than other coils presented in the literature.**

I. Introduction

Wireless power transfer is of great interest for many applications including biomedical, automotive, and consumer handheld electronics [1]–[4]. In many of these applications a high-frequency magnetically-coupled resonant system is the most effective method of transmitting wireless power. The efficiency and range of such a system is limited by the quality factor and coupling coefficient of the resonant coils that generates the electromagnetic coupling [3], [5], [6].

Traditional coils consist of a spiral loop of wire connected to a ceramic or film capacitor. The quality factor of such a coil increases linearly with the diameter of the coil [7], [8]. So we propose a figure of merit Q_d, which is the ratio of the quality factor Q to the diameter d of the coil: $Q_d = \frac{Q}{d}$. Experimental data in the literature for high frequency coils around 6.78 MHz have a Q_d that ranges from 3 to 28 cm^{-1} [3], [9]–[13].

The Q_d of conventional coils is limited by two main factors. First, below 1 MHz coils are typically made from litz wire in order to minimize losses due to skin and proximity effects. However, the benefit of using litz wire is limited in the MHz frequency range due to the need to have strand diameters much smaller than the skin depth. Such small strand diameters are not commercially available because they are difficult and therefore expensive to manufacture. Second, in many designs, eddy currents are induced in the capacitors due to their proximity and orientation to the coil.

To mitigate these issues a multi-layer self-resonant structure using thin sheets of conductors, capacitive ballasting, and low-loss dielectrics was proposed in [14]. This structure consists of alternating layers of C-shape conductors and dielectric rings placed in a ferrite core, creating inductively coupled capacitors in parallel with an inductor. The integration of capacitance in the structure is similar to the integrated LC and LCT (inductor, capacitor, transformer) passive power components discussed in, for example, [15]–[17]. However, unlike the previous work, multi-layer self-resonant structures use the capacitance not only to implement the necessary capacitance, but also to make the conductors more efficient by equalizing current sharing between them. As a result, they not only provide a parts count savings through integration, but also provide a dramatic performance benefit. Furthermore, the self-resonant structure reduces eddy currents by keeping thin foil layers parallel to the magnetic field, and does not require inter-layer connections.

In this work, we present a modification to the self-resonant structure that achieves similar performance, but simplifies the construction process by allowing the thin conductive layers to be constructed from standard PCB substrates. This modification to the self-resonant structure led to the first experimental implementation of a multi-layer self-resonant structure at resonant frequency practical for wireless power transfer.

A related type of self-resonant structure is the split-ring resonator (SRR) [18]. A SRR is a pair of C-shaped conductors that forms a simple resonator which can be arrayed to create metamaterials. Metamaterials can be designed with unusual and controllable electromagnetic properties, and have even been proposed as a way to influence the coupling of resonant inductive wireless power systems. However, although it can be shown that an ideal negative-permeability material could be used to enhance performance, the losses of practical SRRs limit the usefulness of this approach [19]. Whereas an individual SRR comprises just two concentric C-shaped conductors, the self-resonant structure configures them in a stack rather than concentrically, and uses many layers to achieve low losses, in conjunction with soft magnetic material shaping the

field for lowest losses.

The many layers of the self-resonant structure are made from foil, which makes using conductors thinner than the skin depth feasible even at high-frequencies; however, very thin foil layers are difficult to handle. The practical construction challenges associated with using such thin layers prevented us from from experimentally validating the self-resonant structure in [14] at the desired resonant frequency. One way to overcome the challenges associated with using such thin copper layers is to pattern the C-shapes by etching thin copper layers laminated on substrates. In the resonant structure in [14], the capacitance between adjacent conductors, such as those on opposite sides of a substrate, provides the capacitance for resonance. Thus, for high-Q resonance, the substrate dielectric must have a very low dissipation factor. Unfortunately, common substrate materials such as FR4 and polyimide have high dissipation factors (0.015 and 0.002) even at low frequencies and the performance gets worse at higher frequencies. Copper laminates with low-loss substrates such as PTFE are much more expensive.

In this paper, we present a variation of the self-resonant structure described in [14] to allow fabrication with more conventional methods and materials. Our new resonant structure uses high-loss but low-cost substrates such as FR4 and polyimide to support thin conductor layers for easy handling without adversely affecting the quality factor of the resonance. The improved manufacturability of the modified structure presented here allowed us to successfully implement a high-Q 7 MHz resonant structure for wireless power transfer. The modified structure is described in Section II, its loss mechanisms are analyzed in Section III, and experimental characterization results are presented in Section IV.

In addition to wireless power transfer applications, high-Q resonant structures are of interest as passive components for power converter applications. Our design work and test results for similar structures used in resonant power conversion are discussed in [20].

II. Modified Self-Resonant Structure

The modified self-resonant coil is illustrated in Fig. 1. The structure creates a parallel LC resonance. The inductance L is equivalent to a single turn around the magnetic core, while the total capacitance C_{equiv} is created by inductively coupling each section of the structure as shown in the circuit model in Fig. 2. A section of the structure is two C-shaped conductors with opposing orientation that are separated by a low-loss dielectric. For example, in Fig. 1, Layers 2, 3, and 4 form one section. Each section forms two capacitors. One capacitor is formed in each area the conductors overlap as illustrated in Fig. 3. The capacitance between half of one C shape and the facing half of the other C shape in the same section C_{sh}, is a function of the angle of overlap of the layers in radians θ (shown in Fig. 3), the outer radius of the coil r_2, the inner radius r_1, and the dielectric thickness t_d

$$C_{sh} = \frac{\epsilon\theta(r_2^2 - r_1^2)}{t_d 2}. \quad (1)$$

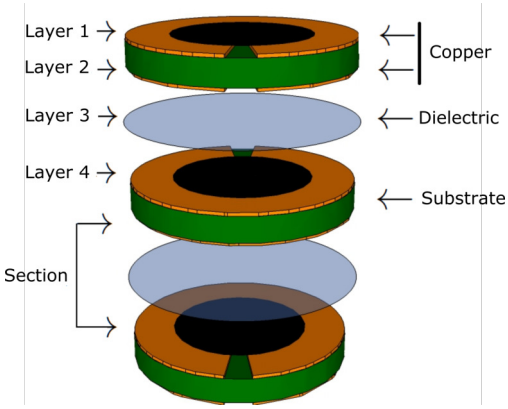

Fig. 1. The layers of a 2 section modified self-resonant structure.

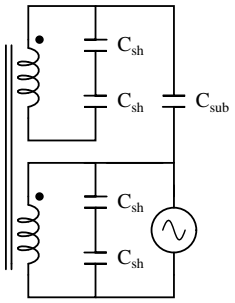

Fig. 2. Equivalent circuit model of a 2 section modified self-resonant structure.

The modified self-resonant structure has m sections, where each section of the structure has two series connected C_{sh}. The equivalent capacitance C_{equiv} of the structure is

$$C_{equiv} = \frac{mC_{sh}}{2}. \quad (2)$$

This is the only capacitance which can be excited, and in conjunction with the inductance determines the resonant frequency of the structure. The resonant frequency of the structure ω_o is given by

$$\omega_o = \frac{1}{\sqrt{LC_{equiv}}}. \quad (3)$$

The proposed modified self-resonant structure allows the

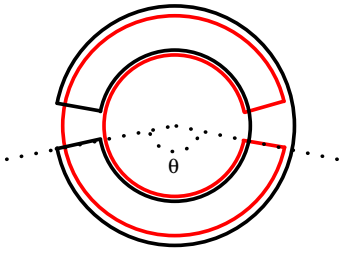

Fig. 3. In this figure two overlapping C-shaped conductors forming one section is shown. Each section forms two capacitors C_{sh} which are connected in series. The angle of overlap of one capacitor θ is marked .

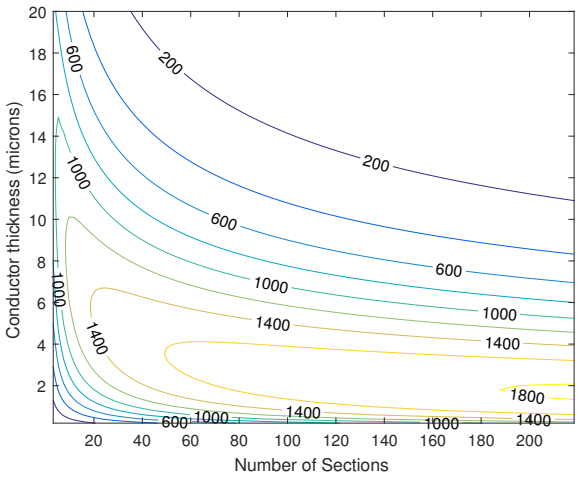

Fig. 4. The theoretical quality factor of the modified self-resonant structure at 7 MHz is plotted as a function of the conductor thickness and the number of sections for a 6.6 cm pot described in Section II. The field weakening factor and current crowding factor are 1 in this figure.

use of low-performance substrates such as FR4 or polyimide without significantly affecting the Q of the structure. To achieve this, any two conductor layers that are separated by a high-loss substrate are oriented such that their gaps are aligned. For example in Fig. 1, the top layer of copper (layer 1) is separated from the second layer of copper (layer 2) by a high-loss substrate, and are both oriented such that the gap is coming out of the page. A capacitance C_{sub} is formed between these two layers; however, the orientation ensures that no strong electric field is generated between the layers. The voltage induced in C_{sub} is only due to the leakage magnetic flux, which is a small fraction of the overall magnetic flux. This allows the high-loss substrate to be integrated into the self-resonant structure, without significantly affecting the quality factor of the structure. Furthermore, the thickness of the substrate does not affect the equivalent capacitance C_{equiv}, so it can be selected based on considerations such as ease of handling, and the overall compactness of the complete structure.

III. Loss Mechanisms

The performance of the modified self-resonant structure is measured by the quality factor of the device at resonance. The quality factor Q is

$$Q = \omega_o L / R_{total}, \tag{4}$$

where R_{total} is sum of 3 equivalent series resistances (ESR) that model winding resistance, core loss, and dielectric loss. The ESR for each of these loss mechanisms is derived in this section.

1) Winding Loss: The power lost in the winding is due to both the low frequency resistance R_{lf} of the winding, and eddy currents due to the high-frequency magnetic field (proximity effect). The increased losses due to these eddy currents can be modeled by a resistance R_e. The power lost in the winding P_{wind} can be expressed as

$$P_{wind} = I_{rms}^2 R_{wind} = I_{rms}^2 R_{lf} + I_{rms}^2 R_e, \tag{5}$$

where R_{wind} is the AC resistance of the structure. Simplification of (5) shows that the AC resistance factor $\frac{R_{ac}}{R_{lf}}$ is $\left(1 + \frac{R_e}{R_{lf}}\right)$. Therefore, the winding resistance of the structure is the product of a low frequency resistance and an AC resistance factor, and is given by

$$R_{wind} = R_{lf}\left(1 + \frac{R_e}{R_{lf}}\right). \tag{6}$$

Both R_{lf} and the AC resistance factor are derived in [14] for the self-resonant structure. The winding resistance is given by

$$R_{wind} = \frac{2\pi\rho}{\ln(\frac{r_2}{r_1})t_c m}\left[k_1 + \frac{m^2}{9}\left(\frac{t_c}{\delta}\right)^4 k_2\right], \tag{7}$$

where k_1 is $(1 - \frac{\theta}{3\pi})$, k_2 is $(1 + \frac{\theta}{\pi})$, t_c is the thickness of the foil layers, δ is the skin depth, and ρ is the resistivity of the conductor material. This analysis assumes that a magnetic core with infinite permeability is placed directly adjacent to the windings. In practice, there is a gap between the magnetic core and the winding, and furthermore the permeability of the high frequency magnetic material is not large enough to be accurately modeled as infinite. Compared to the idealized case, these practical consideration weaken the magnetic field and prevent the magnetic field lines from being perfectly parallel to the foil layers.

The weakening of the magnetic field reduces the power lost due to the proximity effect. The impact of field weakening on the winding resistance is modeled by a field weakening factor F_{fw}. This factor is derived from a finite element analysis described in Appendix A-A. In the idealized case, F_{fw} is 1, and it decreases in practical scenarios. When the magnetic field lines are not parallel to the foil layers horizontal current crowding occurs in the winding. This is modeled with a current crowding factor F_{cc}. This factor is also derived from a finite element analysis, and its extraction process is described in Appendix A-B. In the idealized case F_{cc} is 1, and it increases in practical scenarios. In total the winding resistance is given by

$$R_{wind} = \frac{2\pi\rho}{\ln(\frac{r_2}{r_1})tM}\left[k_1 F_{cc} + \frac{F_{fw}M^2}{9}\left(\frac{t_c}{\delta}\right)^4 k_2\right]. \tag{8}$$

The winding loss expression illuminates important design parameters: the thickness of the conductor and the number of sections. If the conductor is too thick the proximity effect losses will be high, whereas if the conductor is too thin the DC resistance of the conductor will be large. Similarly, an optimal number of sections exists. If too many sections are used, the proximity effect losses will once again be high, and if too few sections are used the conductor resistance will be high. An optimal number of sections and conductor thickness can be derived; however, in our prototyping work, we instead

constrained the design based on material thicknesses that are readily available from stock. A contour plot in Fig. 4 illustrates the impact of varying these parameters on the quality factor of the structure.

2) Magnetic Core Loss: In this application both the real part μ' and the imaginary part μ'' of the magnetic core permeability affect the quality factor of the structure. The loss in the magnetic core is modeled by an ESR, which can be derived from a reluctance model of the magnetic core. Using this model, the single-turn inductance of the structure L^* is a complex number given by

$$L^* = \frac{1}{\frac{\ell_{eh}}{A_e \mu_0 (\mu' - j\mu'')} + \mathscr{R}_a}, \tag{9}$$

where ℓ_{eh} is the effective length of the core half (half the effective length of a full pot core), A_e is the effective area of the core, and $\mathscr{R}_a$ is the reluctance of the air gap. The ESR that models core loss is a function of the angular frequency ω and is given by

$$\begin{aligned} R_{core} &= \Re\left[j\omega L^*\right] \\ &= \frac{\omega \left(\frac{\ell_{eh}}{\mu_0 A_e}\right) \mu''}{\left(\left(\frac{\ell_{eh}}{\mu_0 A_e}\right) + \mathscr{R}_a \mu'\right)^2 + \left(\mathscr{R}_a \mu''\right)^2}. \end{aligned} \tag{10}$$

The denominator of R_{core} is dominated by $\left(\mathscr{R}_a \mu'\right)^2$. Therefore, the ESR of the core is approximately proportional to

$$R_{core} \propto \frac{1}{\mu' Q_{material}}, \tag{11}$$

where the quality factor of the material $Q_{material}$ is $\frac{\mu'}{\mu''}$. In order to reduce core loss, it is important to select a material that both has a large $Q_{material}$, and a large real component of magnetic permeability at the resonant frequency of the structure.

3) Dielectric Loss: The modified self-resonant structure does not use external capacitors, so the loss mechanisms associated with conductors of external capacitors do not impact it. Instead, the losses created by the capacitance C_{equiv} of the structure are due to the dielectric material, and can be modeled with an ESR that is given by

$$R_{dieletrcic} = \frac{D_d}{C_{equiv}\omega}, \tag{12}$$

where D_d is the dissipation factor of the material. To reduce the dielectric loss a material with a small dissipation factor such as PTFE or polypropylene should be used. There are no significant losses created by C_{sub}, despite the use of the high-loss substrate, because it is not involved in the resonance of the structure.

IV. Results - Implementation of the Modified Self-Resonant Structure

The performance of the modified self-resonant structure was experimentally validated. The device comprises three main components. First a pot core was made from Fair-Rite's 67 material. This material was chosen for its low loss at 7 MHz. The pot core has a diameter of 6.6 cm, and a height of 1.62 cm. Next, the conductive layers of the structure were created using 6 μm copper that, for ease of handling, was laminated on both sides of a 25 μm polyimide substrate and patterned into C-shapes using standard PCB fabrication processes. Finally, 50.8 μm thick PTFE film was cut with a die cutter to form the low-loss dielectric layers. A picture of the modified self-resonant structure is shown in Fig. 5, and system parameter values are shown in Table I.

For this implementation of the modified self-resonant structure, the analysis in Section III estimates the ESR of the structure to be 4.9 $\mathrm{m}\Omega$. A finite element analysis of the structure is used to derive the field weakening factor F_{fw} of 0.80, and the current crowding factor F_{cc} of 1.74, which results in a predicted winding resistance of 1.6 $\mathrm{m}\Omega$. Experimentation using FairRite's 67 material found the imaginary component of the relative permeability to be 0.07, which results in an core loss ESR of 1.9 $\mathrm{m}\Omega$. Finally, using the dissipation factor from a PTFE data-sheet, the ESR that model the dielectric loss is 1.4 $\mathrm{m}\Omega$. Given that the inductance of the structure is 155 nH, (4) estimates that this structure will have a quality factor of 1407.

TABLE I
SELF-RESONANT COIL VARIABLES, THEIR DESCRIPTIONS, AND VALUES IN THE EXPERIMENTAL SETUP. THE WINDING, CORE, AND DIELECTRIC ESRS ARE DERIVED FROM THE MODELS IN SECTION III.

Parameter	Description	Value
d	Structure diameter	6.6 cm
m	Number of sections	48
	Core window height	9.2 mm
	Height of structure	16 mm
r_2	Coil outer radius	26.25 mm
r_1	Coil inner radius	14.85 mm
t	Conductor thickness	6 µm
	Substrate thickness	25.4 µm
	Stacked layers height	5.5 mm
θ	Overlap angle	2.97rad
δ	Skin depth	25 µm
ρ	Conductor resistivity	16.8 nΩ-m
F_{fw}	Field Weakening factor	0.80
F_{cc}	Current crowding factor	1.74
R_{wind}	Winding ESR	1.6 mΩ
L	Structure inductance	155 nH
μ'	Core relative permeability	40
μ''	Imaginary relative permeability	0.07
ℓ_{eh}	Effective length of core half	37.5 mm
A_e	Effective core area	717 mm^2
$\mathscr{R}_a$	Reluctance of air path	5.4 $\frac{\mathrm{MA}}{\mathrm{Wb}}$
R_{core}	Core ESR	1.9 mΩ
C_{equiv}	Structure capacitance	3.28 nF
t_d	Dielectric thickness	25.4 µm
ϵ	Dielectric permittivity	$2.2\epsilon_o$
D_d	Dielectric dissipation factor	2×10^{-4}
$R_{dieletric}$	Dielectric ESR	1.4 mΩ

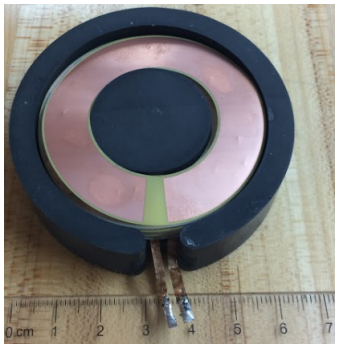

Fig. 5. Picture of the modified self-resonant structure that was used for experimental results.

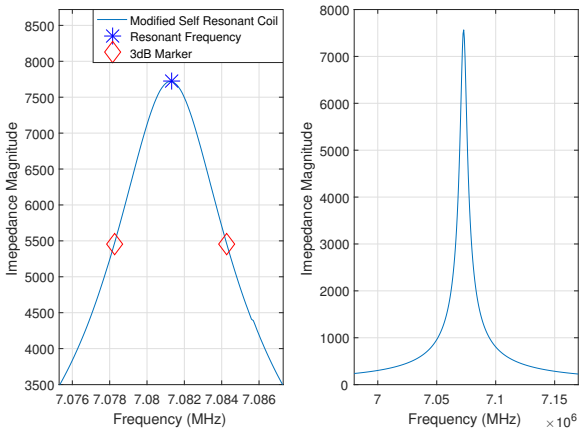

Fig. 6. An Agilent 4294A impedance analyzer was used to measure the impedance magnitude of the modified self-resonant structure around its resonant frequency. The impedance magnitude is shown for two different frequency ranges to illustrate the high-q nature of the resonance. The experimental measured quality factor of the modified self-resonant structure is 1177.

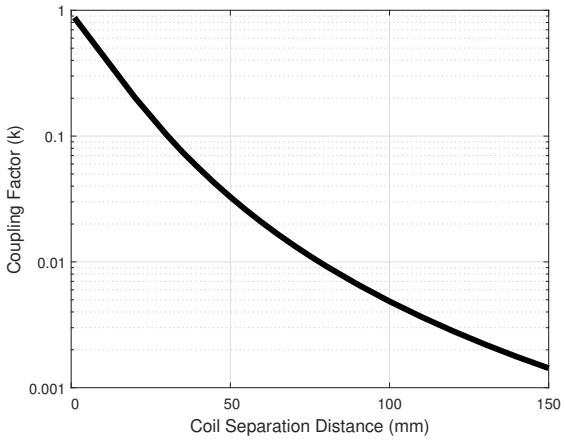

Fig. 7. A finite element analysis is used to derive the coupling coefficient (k) as a function of the distance between the magnetic coils.

A. Experimental Performance of the Modified Self-Resonant Structure

The quality factor of the resonant structure was experimentally found to be 1177. The quality factor was derived from the magnitude of the impedance that is shown in Fig. 6, using the ratio of the resonant frequency to the 3 dB bandwidth. To verify this measurement the quality factor was also derived by measuring inductance, resonant frequency and magnitude of the maximum impedance Z_{pk} to compute $Q = \frac{Z_{pk}}{\omega_o L} = 1136$. The error between the theoretical and experimental quality factor is 16.1%, which suggests good agreement with the analysis presented in Section III. The Q_d of the modified resonant structure is 178 cm^{-1}, which represents a factor of 6.35 improvement over the current state-of-the-art [3], [9]–[13]. The experimental results are summarized in Table II.

TABLE II
SUMMARY OF EXPERIMENTAL RESULTS

Parameter	Description	Value
f_o	Resonant frequency	7.08 MHz
Q	Quality factor	1177
Q_d	Figure of merit (FOM)	178
	FOM percent improvement	635%

B. Impact of the Modified Self-Resonant Structure on Wireless Power Transfer

The maximum achievable efficiency η_{max} between two coils of a wireless power transfer system is dependent on the quality factor Q of the coils, and the coupling coefficient k. The maximum efficiency is derived in [5], [6] and is given by

$$\eta_{max} = \frac{(Qk)^2}{\left(1+\sqrt{1+(Qk)^2}\right)^2}. \tag{13}$$

Therefore, to maximize the efficiency of a wireless power transfer system the quality factor and coupling factor should be maximized.

The modified self-resonant structure has been experimentally demonstrated to have a quality factor that is 6.3 times larger than conventional coils; however, to understand the impact of this on the efficiency of wireless power transfer the coupling factor must also be considered. The coupling factor is determined by the shape, orientation, and properties of the magnetic cores. A finite element analysis of the magnetic core used in this work shows that the coupling factor ranges from 0.875 to 0.0014 as the transmission distance increases from 1 mm to 150 mm. The coupling factor is plotted over this entire range in Fig. 7, and pictures that demonstrate the relative transmission distances compared to the core size are shown in Fig. 8.

The maximum achievable efficiency, given by (13), using the modified self resonant structure is compared to the current state-of-the-art coil designs in Fig 9. For this comparison we assume that each resonator is implemented with the same magnetic core used for our modified self-resonant structure. The maximum achievable efficiency using the modified self-

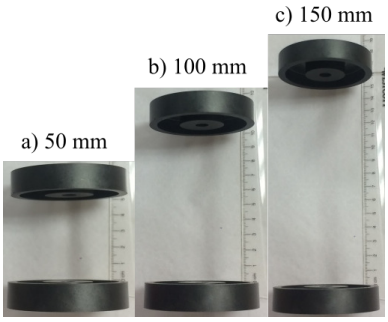

Fig. 8. A picture of the magnetic cores at a separation distances of a) 50 mm, b) 100 mm, and c) 150 mm illustrates the relative size of the coil to the range of wireless power transfer discussed in this work.

resonant structure is derived using the experimental quality factor of 1177 and the simulated coupling factor. The state-of-the-art design uses the same coupling factor as the self-resonant structure, but with a quality factor of 185, which is derived by multiplying the state-of-the-art Q_d by the diameter of the core.

The modified self-resonant structure improves wireless power transfer efficiency for any distance between the coils. For example, if the coils are 20 mm apart the modified self-resonant structure can achieve 98.7% efficiency, while the current state-of-the-art coil coil technology can achieve 91.9%. At longer distances, the difference is even more dramatic. At a distance of 90 mm, the state-of-the-art coil design can only achieve an efficiency of 22%, while the modified self resonant structure achieves an efficiency of 77%. Furthermore the modified self-resonant structure can maintain high efficiency out to longer distances. For example, the modified self resonant structure can maintain at least 90% efficiency at a distance up to 65 mm, while conventional coil designs can only achieve 90% efficiency at distances up to 30 mm.

V. Conclusion

The efficiency and range of resonant wireless power transfer is highly dependent on the quality factor of the resonant tank. This work introduces a new high-Q self-resonant structure that is both easy to manufacture and cost effective. To achieve this goal the thin copper layers of the structure are created using inexpensive substrates such as FR4 or polyimide laminated with copper. Although inexpensive, these substrates are not efficient dielectrics. By orienting the layers on the two sides of the high-loss substrate differently than proposed in [14], we avoid exciting the substrate capacitance and thus avoid losses in it. Experimental results confirm the advantages of the modified self-resonant structure, as the quality factor normalized by the diameter of the structure is shown to be more than 6.35 times higher than the current state-of-the-art without using high-cost materials or manufacturing processes. The improved quality factor of the modified self-resonant structure improves the range over which wireless power can be transferred. For example, compared to the current state-of-the-art, the modified self resonant structure more than double the range at which energy can be transferred at an efficiency of at least 90%.

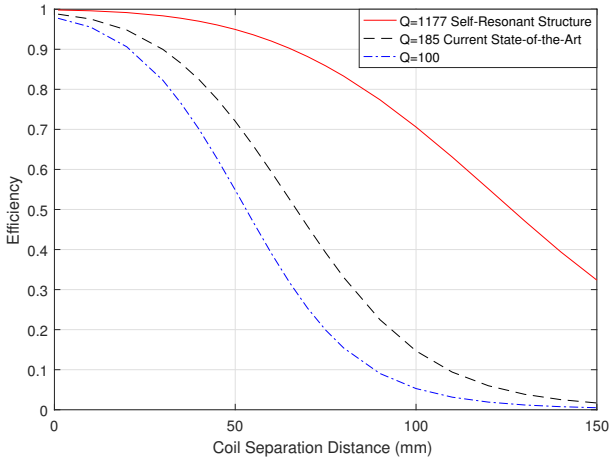

Fig. 9. The theoretical maximum wireless power transfer efficiency as a function of transmission distance is shown for the modified self-resonant structure, and the current state-of-the-art coil design. The drastically improved quality factor of the modified self-resonant structure causes a significant improvement in wireless power transfer efficiency, and improves the viable range of wireless power transfer.

Appendix A
Finite Element Winding Loss Extraction

The field weakening and current crowding factors are extracted from a two-dimensional axisymmetric finite element analysis (FEA). Accurate modeling of the magnetic core properties, and the physical dimensions are important to the result of the simulation. Each section of the modified self resonant structure consists of two copper layers, so the FEA model is an inductor with $2m$ turns of foil. The foil layers of the model are connected in series in order to force equal current sharing between layers, and are driven with an RMS current I_{rms}. The thickness of the foil windings is t_c, and therefore it is important to ensure that the FEA mesh size within the winding is small enough to accurately model the effects within the winding. Finally, a low frequency resistance of the coil R_{lf} is needed for this analysis, and it can be derived from a FEA simulation; however, to reduce computation time an analytical expression is used and is given by

$$R_{lf} = \frac{4m\pi\rho}{\ln\left(\frac{r_2}{r_1}\right)t_c}. \tag{14}$$

A. Field Weakening Factor

The field weakening factor accounts for decreased proximity effect loss due to a reduction in the magnetic field. The proximity effect power loss is produced by the magnetic field inside the winding area; however, the impact of field weakening is derived by only considering the spatial average of the square of the peak value of the magnetic field parallel to

the foil layers $\left\langle \hat{B}_r^2 \right\rangle$. The power loss due to the parallel-flux proximity effect P_{prox} is given by

$$P_{prox} = \frac{\left\langle \hat{B_r}^2 \right\rangle \omega^2 t_c^2}{24\rho} V_f \tag{15}$$

where V_f is the total volume of the foil. F_{fw} is derived by equating the AC resistance calculated with the simulated field strength $(1 + \frac{P_{prox}}{I_{rms}^2 R_{lf}})$ to the theoretical AC resistance factor $(1 + F_{fw}\frac{(2m)^2}{9}\left(\frac{t_c}{\delta}\right)^4)$. The field weakening factor is derived from this relationship and is given by

$$F_{fw} = \frac{9P_{prox}}{I_{rms}^2 R_{lf} (2m)^2 \left(\frac{t_c}{\delta}\right)^4}. \tag{16}$$

B. Current Crowding Factor

The current crowding factor accounts for increased losses in the conductors due to horizontal current crowding. This factor is derived from the resistance R_{fea} of the FEA model at the resonant frequency. The ratio of R_{fea} to R_{lf} is

$$\frac{R_{fea}}{R_{lf}} = \frac{F_{fw}(2m)^2}{9}\left(\frac{t_c}{\delta}\right)^4 + F_{cc}, \tag{17}$$

so the current crowding factor F_{cc} is given by

$$F_{cc} = \frac{R_{fea}}{R_{lf}} - \frac{F_{fw}(2m)^2}{9}\left(\frac{t_c}{\delta}\right)^4. \tag{18}$$

REFERENCES

[1] J. S. Ho, A. J. Yeh, E. Neofytou, S. Kim, Y. Tanabe, B. Patlolla, R. E. Beygui, and A. S. Poon, "Wireless power transfer to deep-tissue microimplants," *Proceedings of the National Academy of Sciences*, vol. 111, no. 22, pp. 7974–7979, 2014.

[2] M. Adeeb, A. Islam, M. Haider, F. Tulip, M. Ericson, and S. Islam, "An inductive link-based wireless power transfer system for biomedical applications," *Active and Passive Electronic Components*, 2012.

[3] A. P. Sample, D. A. Meyer, and J. R. Smith, "Analysis, experimental results, and range adaptation of magnetically coupled resonators for wireless power transfer," *IEEE Transactions on Industrial Electronics*, vol. 58, no. 2, pp. 544–554, 2011.

[4] T. Imura, H. Okabe, and Y. Hori, "Basic experimental study on helical antennas of wireless power transfer for electric vehicles by using magnetic resonant couplings," in *Vehicle Power and Propulsion Conference*. IEEE, 2009, pp. 936–940.

[5] E. Waffenschmidt and T. Staring, "Limitation of inductive power transfer for consumer applications," in *13th European Conference on Power Electronics and Applications*. IEEE, 2009, pp. 1–10.

[6] M. Kesler, "Highly resonant wireless power transfer: Safe efficient, and over distance," *Witricity Corporation*, pp. 1–32, 2013.

[7] C. R. Sullivan, B. A. Reese, A. L. Stein, and P. A. Kyaw, "On size and magnetics: Why small efficient power inductors are rare," in *3D Power Electronics Integration and Manufacturing (3D-PEIM), International Symposium on*. IEEE, 2016, pp. 1–23.

[8] D. J. Perreault, J. Hu, J. M. Rivas, Y. Han, O. Leitermann, R. C. Pilawa-Podgurski, A. Sagneri, and C. R. Sullivan, "Opportunities and challenges in very high frequency power conversion," in *Applied Power Electronics Conference and Exposition*. IEEE, 2009, pp. 1–14.

[9] K. Fotopoulou and B. W. Flynn, "Wireless power transfer in loosely coupled links: Coil misalignment model," *IEEE Transactions on Magnetics*, vol. 47, no. 2, pp. 416–430, 2011.

[10] C. Florian, F. Mastri, R. P. Paganelli, D. Masotti, and A. Costanzo, "Theoretical and numerical design of a wireless power transmission link with GaN-based transmitter and adaptive receiver," *IEEE Transactions on Microwave Theory and Techniques*, vol. 62, no. 4, pp. 931–946, 2014.

[11] A. Khripkov, W. Hong, and K. Pavlov, "Design of an integrated resonant structure for wireless power transfer and data telemetry," in *Microwave Workshop Series on RF and Wireless Technologies for Biomedical and Healthcare Applications (IMWS-BIO)*. IEEE, 2013, pp. 1–3.

[12] A. Kurs, A. Karalis, R. Moffatt, J. D. Joannopoulos, P. Fisher, and M. Soljačić, "Wireless power transfer via strongly coupled magnetic resonances," *Science*, vol. 317, no. 5834, pp. 83–86, 2007.

[13] S.-H. Lee and R. D. Lorenz, "Development and validation of model for 95%-efficiency 220 watt wireless power transfer over a 30-cm air gap," *IEEE Transactions on Industry Applications*, vol. 47, no. 6, pp. 2495–2504, 2011.

[14] C. R. Sullivan and L. Beghou, "Design methodology for a high-Q self-resonant coil for medical and wireless-power applications," in *14th Workshop on Control and Modeling for Power Electronics (COMPEL)*. IEEE, 2013, pp. 1–8.

[15] J. A. Ferreira and J. D. Van Wyk, "Electromagnetic energy propagation in power electronic converters: toward future electromagnetic integration," *Proceedings of the IEEE*, vol. 89, no. 6, pp. 876–889, 2001.

[16] J. T. Strydom and J. D. Van Wyk, "Volumetric limits of planar integrated resonant transformers: a 1 MHz case study," *IEEE Transactions on Power Electronics*, vol. 18, no. 1, pp. 236–247, 2003.

[17] E. Waffenschmidt and J. Ferreira, "Embedded passives integrated circuits for power converters," vol. 1, 2002, pp. 12–17.

[18] R. Marques, J. Martel, F. Mesa, and F. Medina, "Left-handed-media simulation and transmission of EM waves in subwavelength split-ring-resonator-loaded metallic waveguides," *Physical Review Letters*, vol. 89, no. 18, p. 183901, 2002.

[19] T. Oh and B. Lee, "Analysis of wireless power transfer using metamaterial slabs made of ring resonators at 13.56 mhz," *Journal of electromagnetic engineering and science*, vol. 13, no. 4, pp. 259–262, 2013.

[20] P. Kyaw, A. Stein, and C. R. Sullivan, "High-Q resonator with integrated capacitance for resonant power conversion," in *Applied Power Electronics Conference and Exposition*. IEEE, 2016.